

STREAMING MOTIONS TOWARDS THE SUPERMASSIVE BLACK HOLE IN NGC 1097

KAMBIZ FATHI

Physics Department, Rochester Institute of Technology, 85 Lomb Memorial Dr., Rochester, New York 14623, USA

THAISA STORCHI-BERGMANN & ROGEMAR A. RIFFEL

Instituto de Física, UFRGS, Av. Bento Goncalves 9500, 91501-970 Porto Alegre RS, Brazil

CLAUDIA WINGE

Gemini Observatory, c/o AURA Inc., Casilla 603, La Serena, Chile

DAVID J. AXON & ANDREW ROBINSON

Physics Department, Rochester Institute of Technology, 85 Lomb Memorial Dr., Rochester, New York 14623, USA

ALESSANDRO CAPETTI

INAF - Osservatorio Astronomico di Torino, Strada Osservatorio 20, 10025 Pino Torinese, Italy

ALESSANDRO MARCONI

INAF - Osservatorio Astrofisico di Arcetri, Largo Fermi 5, I-50125 Firenze, Italy

Accepted for publication in ApJ Letters

ABSTRACT

We have used GMOS-IFU and high resolution HST-ACS observations to map, in unprecedented detail, the gas velocity field and structure within the 0.7 kpc circumnuclear ring of the SBb LINER/Seyfert 1 galaxy NGC 1097. We find clear evidence of radial streaming motions associated with spiral structures leading to the unresolved (< 3.5 parsecs) nucleus, which we interpret as part of the fueling chain by which gas is transported to the nuclear starburst and supermassive black hole.

Subject headings: Galaxies: active, Galaxies: kinematics and dynamics, Galaxies: nuclei

1. INTRODUCTION

Mechanisms of mass transfer in active galaxies from galactic scales down to nuclear scales, have been the subject of many theoretical and observational studies (e.g., Shlosman, Begelman, & Frank 1990; Emsellem, Goudfrooij, & Ferruit 2003; Knapen 2005). Simulations have shown that non-axisymmetric potentials efficiently promote gas inflow towards the inner kpc-scale regions (e.g., Engelmaier & Shlosman 2004). Further, recent observations have revealed that structures such as small-scale disks or nuclear bars and associated spiral arms are frequently observed in the inner regions of active galaxies, suggesting they could be the means to transport gas from the kpc scale down to within a few tens of parsecs of the active nucleus (e.g., Knapen et al. 2000; Emsellem et al. 2001; Maciejewski et al. 2002; Crenshaw, Kraemer, & Gabel 2003; Fathi et al. 2005).

The nearby (14.5Mpc) LINER/Sey 1 galaxy NGC 1097 is an important “laboratory” in this context. It hosts a large-scale bar as well as a secondary bar within its 0.7 kpc circumnuclear ring (e.g., Shaw et al. 1993). Since the discovery of its double peaked H α emission-lines (Storchi-Bergmann, Baldwin, & Wilson 1993), there have been several studies to follow the “fate” of the gas accumulated in the centre (e.g., Storchi-Bergmann et al. 2003).

Recently Prieto, Maciejewski, & Reunanen (2005;

henceforth PMR05) have presented high resolution ground-based near-infrared images obtained with the Very Large Telescope. They reported the discovery of spiral structures within the inner 300 pc of the galaxy, which can be traced to within ≈ 10 pc of the nucleus (the limit of their spatial resolution). PMR05 argued that these spirals trace cool dust, and could be channels by which cold gas and dust are flowing to the nuclear supermassive black hole (hereafter SMBH).

Here we present two-dimensional maps of the gas kinematics and structure within the inner 0.5×1.0 kpc of NGC 1097, which appear to trace the fueling path to the unresolved nucleus. Our study is based on high signal-to-noise ratio spectra obtained with the Gemini Multi Object Spectrograph (GMOS-S) Integral Field Unit (IFU), which reveal the inner gas kinematics in unprecedented detail. We use these data in combination with high resolution images obtained with the Advanced Camera for Surveys of the Hubble Space Telescope (HST-ACS) to cross-correlate the gas kinematics with the morphology of the nuclear spiral structure.

2. OBSERVATIONS

Our two-dimensional spectroscopic observations of NGC 1097 were obtained with the GMOS-IFU on the Gemini South Telescope, on January the 8th 2005, using the R400_G5325 grating and r_G0326 filter (Gemini project GS-2004B-Q-25, PI: Storchi-Bergmann). These spectra cover the wavelength range 5600-7000 Å at a

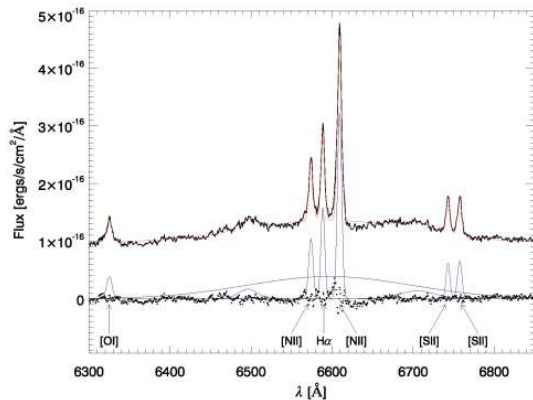


FIG. 1.— Sample GMOS spectrum of the nucleus illustrating the multi-Gaussian fit used to determine the velocities of the narrow lines and remove the underlying double-peaked broad H-alpha line. Each of the labelled narrow lines is modelled by a single Gaussian profile. The broad H-alpha line is represented by the 3 broader Gaussians. The individual Gaussian components are plotted below the spectrum, together with the residuals (dots) resulting from a simultaneous fit to the spectrum of all the Gaussians plus a fixed continuum level. The three “unmarked” Gaussians are a fit simply to remove nuisance structure due to the double-peaked broad H α emission-line.

spectral resolution of $R \approx 3500$ (85 km s^{-1} FWHM). We observed three consecutive fields of angular dimensions $5'' \times 7''$ each, covering in total $15''$ along the major axis of the galaxy (position angle $PA=129^\circ$) and $7''$ along the minor axis, sampled by hexagonal lenslets with projected diameters of $0''.2$. Three exposures of 600 seconds were obtained for each field, slightly shifted along $PA=40^\circ$ in order to correct for detector defects. The spectra were reduced using standard tasks in IRAF. Products of the reductions are three wavelength and flux-calibrated data cubes, resampled to rectangular arrays of 50×70 spectra, each corresponding to an angular coverage of $0''.1 \times 0''.1$.

The HST-ACS image for NGC 1097 was obtained (GO 9782; PI: Axon) using the HRC mode ($0''.025 \text{ pix}^{-1}$ and a field of view of $26'' \times 29''$), through the FR656N filter. The ACS image was reduced and flux calibrated using the standard CALACS pipeline.

3. RESULTS

3.1. Spectroscopy

We used the two-dimensional spectroscopic observations to map the kinematics of the ionized gas in the central $0.5 \times 1 \text{ kpc}$. Inspection of the individual spectra reveals the presence of the [O I] $\lambda\lambda 6300, 6364$, H $\alpha\lambda 6563$, [N II] $\lambda\lambda 6548, 6583$, and [S II] $\lambda\lambda 6717, 6731$ emission-lines throughout most of the observed field. The velocity field was derived from the central wavelengths of Gaussians fitted to the narrow H α component and to the [N II] emission-lines, as these lines have good signal-to-noise ratio even at the borders of the fields. Within the inner $0''.5$, we introduced 3 additional Gaussian components to fit and remove the underlying double-peaked broad component of the H α line (see for example, Fig. 1). However, this does not significantly affect the velocity field derived from the narrow lines. Since the velocity fields of H α and [N II] $\lambda 6583$ are identical within the uncertainties ($\approx 10 \text{ km s}^{-1}$), we chose the latter to represent the gaseous velocity field of the galaxy because of its higher signal-to-noise ratio.

In the top panels of Fig. 2, we present the two-dimensional maps of the total flux in the bandpass, the integrated [N II] $\lambda 6583$ flux, and velocity dispersion (σ). The nucleus is at position (0, 0), while a part of the circumnuclear 0.7 kpc star-forming ring is visible at the top of the panels. The σ map (corrected for the instrumental resolution) has circumnuclear values around 40 km s^{-1} and decrease outwards to values of $\approx 15 \text{ km s}^{-1}$, as one approaches the circumnuclear ring at about $7''$ south-east from the nucleus.

The velocity field is shown in the bottom left panel of Fig. 2. It is clearly dominated by rotation with distortions indicative of significant non-circular motions. Similar distortions have previously been observed in the large-scale gas kinematics of nearby disk galaxies (e.g. Visser 1980; Zurita et al. 2004; Emsellem et al. 2006), where they were found to trace the galaxy spiral arms. In order to try to isolate these non-circular motions we have fitted an exponential thin disk model (Freeman 1970) to the velocity field using a method developed by Fathi (2004). In the bottom middle panel of Fig. 2, we illustrate the best model, which has a deprojected maximum amplitude of $\approx 200 \text{ km s}^{-1}$, a disk scale length of $3''.5$, a kinematic PA of 137° and disk inclination of 35° . This inclination is similar to that derived by Storchi-Bergmann et al. (2003) for the nuclear accretion disk, but is smaller than the value of 46° found from the large-scale gas kinematics by Storchi-Bergmann et al. (1996). The kinematic PA agrees with the value of 135° from Storchi-Bergmann et al. (1996) and Emsellem et al. (2001). We have tested the robustness of the model against extinction variations across the field by repeating the fit several times, masking out the regions most affected by the distortions. We found no significant variations in the model parameters.

We constructed a residual map by removing the disk model from the observed velocity field. The result is shown in the bottom right panel of Fig. 2, where it can be observed that the residuals display amplitudes of $\approx 50 \text{ km s}^{-1}$. Moreover, the velocity residuals are distributed in a spiral pattern, centered on the nucleus. We identify three main arms, designated 1, 2, and 3, which are outlined by white dots superposed on the residual map. The residuals indicate redshifts along arm 2, but blueshifts along arms 1 and 3. As arms 1 and 2 are oriented approximately along the minor axis, and the south-west is the near side of the galaxy (Storchi-Bergmann et al. 1996), we conclude that the residuals indicate radial inflow of gas along these circumnuclear arms. This follows from the geometry of a configuration where the radial motions occur along the spiral arms which are in the plane of the disk. In this case, one expects the maximum line-of-sight velocities along the minor axis. Furthermore, this implies that the spiraling direction is clockwise. This simple setup does not fully explain the observed blueshift along the inner parts of arm 3, where outflows or individual gas clouds could complicate the observed velocities.

3.2. Imaging

We used two different techniques of image analysis to investigate the structures present in the image. The first is generating a “structure map”, which is based on the Richardson-Lucy image restoration technique (e.g.,

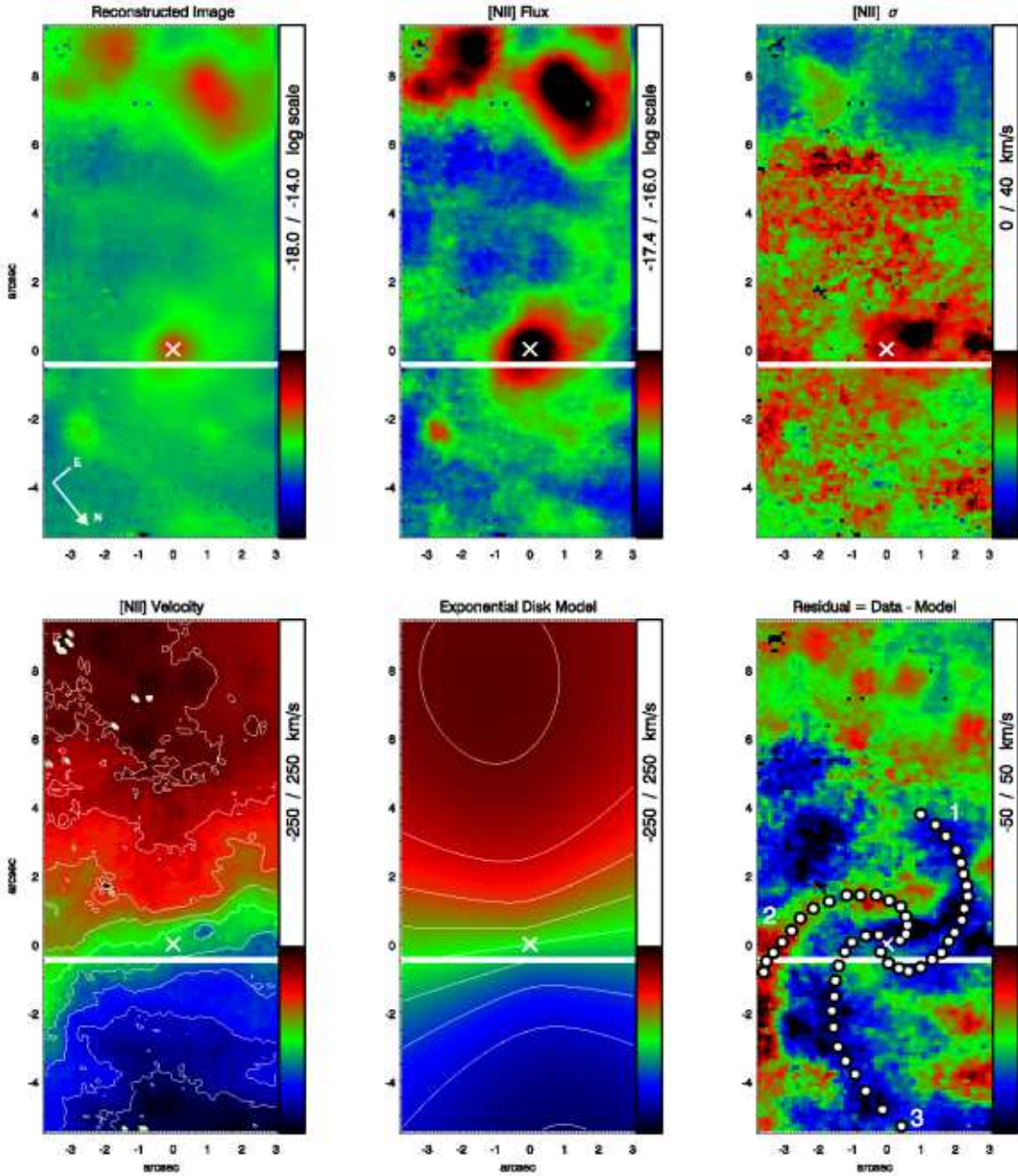


FIG. 2.— GMOS-IFU data results: Reconstructed image formed by collapsing the 6300-6850 Å wavelength range (top left); [N II] λ 6583 Flux distribution (top middle); together with the kinematic maps derived from the [N II] λ 6583 emission-line, as well as the best fitting exponential disk velocity field model and residuals. The spiral features are delineated by white dots, with the numbers indicating the different arms as in Fig. 3. In the bottom panels, red color indicates redshift and blue color, blueshift. All panels share the same orientation.

Pogge & Martini 2002). The second method we have applied for enhancing the morphological structures makes use of the IRAF STSDAS/ELLIPSE ellipse fitting routine to construct a model for the galaxy. The structures are revealed in the residual image obtained by subtracting the model from the original image (see Fig. 3).

The original ACS image shows several dark filaments, in the form of spirals, which are enhanced in the processed images. A comparison with the J-band image of PMR05 (their Fig. 5), shows good agreement between the spiral structures seen in the optical and near-infrared, and supports their interpretation that the dark filaments map dust spirals which converge on the unresolved nucleus. The dark filaments form a pattern similar to that seen in the velocity residuals. However, a detailed com-

parison of the velocity residual map with the ACS image shows that the spiral structure identified in the former is rotated relative to that traced by the dark filaments in the latter. To illustrate this, we have overplotted the loci of the velocity residual spiral arms on the ACS image (Fig. 3). The radial streaming motions in the ionized gas occur *between* the spiral dust lanes. The latter are indicated by white crosses in Fig. 3.

4. CONCLUSIONS

We have mapped the gas velocity field in the inner $7'' \times 15''$ of NGC 1097 with GMOS-IFU at an unprecedented spatial resolution. These data have enabled us to disentangle circular from non-circular motions in the ionized gas. The dominant motion is disk rotation, upon

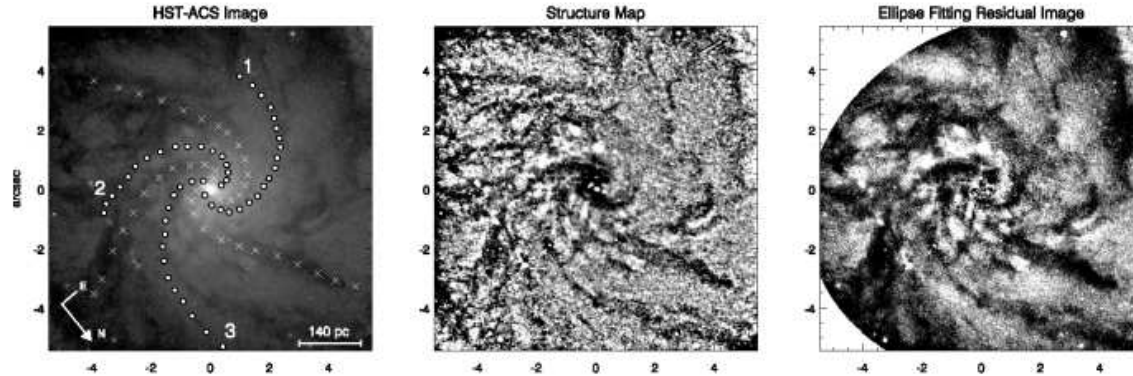


FIG. 3.— The inner $10'' \times 10''$ of the HST-ACS image of NGC 1097 (left), the structure map (middle), and residual between the HST image and the elliptical model (right). The angular sampling of $0''.025 \text{ pix}^{-1}$ corresponds to $\approx 1.8 \text{ pc pix}^{-1}$ at the galaxy. The dots delineate the spiral arms found in our kinematic analysis, labeled as in Fig. 2, which follow clockwise rotation (see Sec. 3.1). The white crosses mark the dark regions from Fig. 5 of PMR05.

which are superimposed velocity residuals that delineate three spiral arms converging onto the unresolved nucleus. We interpret the residual velocities - which reach $\approx 20\%$ of the rotational velocity amplitude - as evidence for radial inflow at $\approx 50 \text{ km s}^{-1}$ from the region interior to the circumnuclear 0.7 kpc ring, towards the nucleus.

A similar spiral structure delineated by dust lanes is seen in both our optical HST-ACS image and the near-infrared images of PRM05. The radial streaming motions in the ionized gas occur between the spiral dust lanes. On larger scales, similar displacements between gas and dust are common in galactic spiral arms (Tilanus & Allen 1991). This offset is attributed to loss of angular momentum of the gas as it passes through the spiral shock (e.g., Combes 1996). Assuming that the dust lanes trace the spiral shock, a similar mechanism may operate in the inner kpc of NGC 1097. As gas initially on circular orbits passes through the shock, some fraction of its kinetic energy is thermalized, it loses angular momentum and falls toward the center of the gravitational potential.

Taken at face value, the inferred streaming velocities would bring the gas from scales of 10 pc (the spatial resolution of our kinematic maps) down to the nuclear SMBH in approximately 200,000 yrs. Such a gas flow could also be responsible for triggering the recently discovered starburst activity in the immediate vicinity of the nucleus (Storchi-Bergmann et al. 2005).

NGC 1097 seems to have all the necessary features to

allow gas transfer from galactic scales down to the nucleus (e.g., Engelmaier & Shlosman 2004; Maciejewski 2004). It has a large-scale bar, which is most likely the agent to bring gas down to the well known circumnuclear ring. It has a secondary bar, which further funnels gas toward the nuclear region, while here we have mapped streaming velocities along spiral structures, down to at least 10 pc from the nucleus. Further, the high resolution HST-ACS image suggests that these structures continue down to $\approx 3.5 \text{ pc}$ scale. It is the first time that radial gas inflow has been mapped to such small radii from the central supermassive black hole.

Based on observations with the NASA/ESA Hubble Space Telescope (HST-GO 09782.01) obtained at the Space Telescope Science Institute, which is operated by the Association of Universities for Research in Astronomy, Inc., under NASA contract NAS5-26555. Also based on observations obtained at the Gemini Observatory, operated by the Association of Univ. for Research in Astronomy, Inc., under a cooperative agreement with the NSF on behalf of the Gemini partnership: the NSF (USA), the PPARC (UK), the National Research Council (Canada), CONICYT (Chile), the Australian Research Council (Australia), CNPq (Brazil) and CONICET (Argentina). T. Storchi-Bergmann acknowledges support from the Brazilian institution CNPq.

REFERENCES

- Combes, F. 1996, in IAU Colloq. 157, Barred Galaxies, ed. R. Buta, D. A. Crocker, & B. G. Elmegreen (San Francisco: ASP), 286
- Crenshaw, D. M., Kraemer, S. B., Gabel, J. R. 2003, *AJ*, 126, 1690
- Emsellem, E., Greusard, D., Combes, F., Friedli, D., Leon, S., Pécontal, E., Wozniak, H. 2001, *A&A*, 368, 52
- Emsellem, E., Goudfrooij, P., Ferruit, P. 2003, *MNRAS*, 345, 1297
- Emsellem, E., Fathi, K., Wozniak H., Ferruit, P., Mundell, C. G., Shinnerer, E. 2006, *MNRAS*, 365, 367
- Engelmaier, P., Shlosman, I. 2004, *ApJ*, 617, L115
- Fathi, K. 2004, Ph.D. Thesis, University of Groningen
- Fathi, K., et al. 2005, *MNRAS*, 364, 773
- Freeman, K. C. 1970, *ApJ*, 160, 811
- Knapen, J. H., Shlosman, I., Heller, C. H., Rand, R. J., Beckman, J. E., Rozas, M. 2000, *ApJ*, 528, 219
- Knapen, J. H. 2005, *Ap&SS*, 295, 85
- Maciejewski, W., Teuben, P. J., Sparke, L. S., Stone, J. M. 2002, *MNRAS*, 329, 502
- Maciejewski, W. 2004, *MNRAS*, 354, 883
- Pogge, R. W., Martini, P. 2002, *ApJ*, 569, 624
- Prieto, M. A., Maciejewski, W., Reunanen, J. 2005, *ApJ*, 130, 1472
- Shaw, M. A., Combes, F., Axon, D. J., Wright, G. S. 1993, *A&A*, 273, 31
- Shlosman, I., Begelman, M. C., Frank, J. 1990, *Nature*, 345, 679
- Storchi-Bergmann, T., Baldwin, J. A., Wilson, A. S. 1993, *ApJ*, 410, L11
- Storchi-Bergmann, T., Rodriguez-Ardila, A., Schmitt, H. R., Wilson, A. S., Baldwin, J. A. 1996, *ApJ*, 472, 83
- Storchi-Bergmann, T., et al. 2003, *ApJ*, 598, 956
- Storchi-Bergmann, T., et al. 2005, *ApJ*, 624, L13
- Tilanus, R. P. J. & Allen, R. J. 1991, *A&A*, 244, 8
- Visser, H. C. D. 1980, *A&A* 88, 159
- Zurita, A., Relaño, M., Beckman, J. E., Knapen, J. H. 2004, *A&A*, 413, 73